



Contents lists available at ScienceDirect

Mutat Res Gen Tox En

journal homepage: www.elsevier.com/locate/gentox

Kidney nanotoxicity studied in human renal proximal tubule epithelial cell line TH1

Monika Sramkova^{a,*}, Katarina Kozics^a, Vlasta Masanova^b, Iveta Uhnakova^b, Filip Razga^{c,i}, Veronika Nemethova^{c,i}, Petra Mazancova^{c,i}, Lucyna Kapka-Skrzypczak^{d,e}, Marcin Kruszewski^{d,e,f}, Marta Novotova^g, Victor F. Puentes^h, Alena Gabelova^a

^a Cancer Research Institute, Biomedical Research Center SAS, Dubravská cesta 9, 845 05, Bratislava, Slovakia

^b Slovak Medical University, Limbova 12, 833 03, Bratislava, Slovakia

^c Polymer Institute SAS, Dubravská cesta 9, 845 41, Bratislava, Slovakia

^d Department of Molecular Biology and Translational Research, Institute of Rural Health, Jaczewskiego 2, 20-090, Lublin, Poland

^e Department of Medical Biology and Translational Research, Faculty of Medicine, University of Information Technology and Management, Suchbátskiego 2, 35-225, Rzeszów, Poland

^f Centre for Radiobiology and Biological Dosimetry, Institute of Nuclear Chemistry and Technology, Dorodna 16, 03-195, Warsaw, Poland

^g Institute of Experimental Endocrinology, Biomedical Research Center SAS, Dubravská cesta 9, 845 05, Bratislava, Slovakia

^h Catalan Institute of Nanoscience and Nanotechnology (ICN2), CSIC and BIST, Campus UAB, Bellaterra, 08193, Barcelona, Spain

ⁱ Selecta Biotech SE, Heydukova 2138/1, 811 08, Bratislava, Slovakia

ARTICLE INFO

Keywords:

Inorganic nanoparticles
Human renal proximal tubule cells
Comet assay
TEM analysis
AAS analysis
ICP-MS

ABSTRACT

Progressive expansion of nanomaterials in our everyday life raises concerns about their safety for human health. Although kidneys are the primary organs of xenobiotic elimination, little attention has been paid to the kidneys in terms of nanotoxicological studies up to now. Here we investigate the cytotoxic and genotoxic potential of four solid-core uncoated inorganic nanoparticles (TiO₂NPs, SiO₂NPs, Fe₃O₄NPs and AuNPs) using the human renal proximal tubule epithelial TH1 cells. To mimic the *in vivo* conditions more realistic, TH1 cells were exposed *in vitro* to inorganic NPs under static as well as dynamic conditions for 3 h and 24 h. The medium throughput alkaline comet assay (12 minigels *per* slide) was employed to evaluate the impact of these NPs on genome integrity and their capacity to produce oxidative lesions to DNA. The accumulation and localization of studied inorganic NPs inside the cells was monitored by transmission electron microscopy (TEM) and the efficacy of internalization of particular NPs was determined by atomic absorption spectroscopy (AAS) and inductively coupled plasma mass spectrometry (ICP-MS). From all the tested NPs, only Fe₃O₄NPs induced a slight cytotoxicity in TH1 cells exposed to high concentrations (> 700 µg/ml) for 24 h. On the other hand, the inorganic NPs did not increase significantly the level of DNA strand breaks or oxidative DNA damage regardless of the treatment mode (static vs. dynamic conditions). Interestingly, substantial differences were observed in the internalized amount of inorganic NPs in TH1 cells exposed to equivalent (2.2 µg/ml) concentration. Fe₃O₄NPs were most efficiently taken up while the lowest quantity of particles was determined in TiO₂NPs-treated cells. As the particle size and shape of individual inorganic NPs in culture medium was nearly identical, it is reasonable to suppose that the chemical composition may contribute to the differences in the efficacy of NPs uptake.

1. Introduction

The kidneys are vital organs that perform several important physiological functions such as regulation of blood pressure, control of plasma concentrations of nutrients and electrolytes, reabsorption of water and small molecules, production of hormones, as well as detoxification and excretion of xenobiotics from the body [1,2]. High blood

supply and ability to concentrate toxins, makes the kidneys particularly susceptible to xenobiotics, including nanoparticles (NPs), which reach the bloodstream after intentional or unintentional exposure. Generally, liver and kidneys are the most common accumulation secondary organs regardless of exposure routes, animal models and physicochemical properties of NPs [3]. In comparison to lungs, the most important target organ in the case of occupational exposure [4], the impact of NPs in

* Corresponding author.

E-mail address: monika.sramkova@savba.sk (M. Sramkova).

<https://doi.org/10.1016/j.mrgentox.2019.01.012>

Received 26 July 2018; Received in revised form 27 November 2018; Accepted 17 January 2019

1383-5718/ © 2019 The Authors. Published by Elsevier B.V. This is an open access article under the CC BY-NC-ND license (<http://creativecommons.org/licenses/by-nc-nd/4.0/>).

kidneys has though received only little attention. So far, limited number of *in vitro* and *in vivo* studies has proved the capacity of NPs to exert various adverse effects on kidneys, thus affecting their physiological functions [5]. Among them, mainly metal NPs and silica, have been already shown to induce nephrotoxicity and different levels of adverse renal effects [6–13]. However, up to the date there are no validated or regulatory approved *in vitro* models available for predicting nephrotoxicity, which means there is still a great need for the development of new *in vitro* renal cell models.

Renal clearance of waste products and xenobiotics is a multifaceted process involving glomerular filtration, tubular reabsorption and secretion, and elimination of the compound through urinary excretion, thus employing all the kidney compartments. Differences in the impact of NPs on particular nephron structure, the basic structural and functional unit of the kidney, have been detected (reviewed in Du et al., 2018). For example, signs of glomerulonephritis have been observed in mice after exposure to 25 nm and 80 nm TiO₂NPs [12] as well as 23.5 nm CuNPs [6], both applied by oral gavage. On the other hand, no significant changes in the glomeruli were found after exposure of mice to various sizes of AuNPs (10, 20, 50 nm, i.p. exposure) [13]. In contrast to glomeruli alterations upon NPs exposure, structural changes (renal fibrosis) and pathological degeneration within the renal proximal convoluted tubules have been determined in mice exposed to TiO₂NPs and CuNPs [6,12]. These results indicated that the tubular region of the kidneys might be a preferential site of NPs toxicity. This suggestion supports the fact that a greater sensitivity of tubular LLC-PK1 cells compared to mesangial IP15 cells was detected *in vitro* after treatment with carbon black nanoparticles and TiO₂NPs [14]. Moreover, experiments on rats revealed that even the proximal renal convoluted tubules are more susceptible to AuNPs toxicity than the distal ones [13].

Therefore, the aim of this study was evaluate the nephrotoxicity of four inorganic solid-core uncoated NPs using immortalized human renal proximal tubule epithelial TH1 cell line which displays several characteristics of the proximal tubule [15]. Tested NPs (titanium dioxide/TiO₂NPs, silica dioxide/SiO₂NPs, magnetite/Fe₃O₄NPs and gold nanoparticles/AuNPs) are routinely used in biomedical applications or consumer products. The proximal tubule epithelial cells are naturally exposed to fluid shear stress generated by continuously filtrate movement from glomeruli to urinary bladder. In order to more realistically recapitulate the *in vivo* conditions, TH1 cells were *in vitro* exposed to model inorganic NPs under static as well as dynamic conditions. The cytotoxicity of selected inorganic NPs was evaluated by alamarBlue® assay and the alkaline comet assay was used to investigate their impact on genome integrity and capacity to induce oxidative DNA lesions. Intracellular localization of NPs and ultrastructural changes in morphology of TH1 cells upon NPs treatment were studied by transmission electron microscopy (TEM) and the internalized amount of particular inorganic NPs inside the cells was determined by flame atomic absorption spectroscopy (FAAS) and inductively coupled plasma mass spectrometry (ICP-MS).

2. Materials and methods

2.1. Chemicals

Ethidium bromide (EtBr), low-melting-point (LMP) agarose, normal-melting-point (NMP) agarose, Triton X-100, and HEPES were purchased from Sigma-Aldrich (Lambda Life, Slovakia), and formamidopyrimidine-DNA glycosylase/AP nuclease (Fpg) was purchased from New England Biolabs (BioTech, Slovakia). (R)-1-[(10-Chloro-4-oxo-3-phenyl-4H-benzo(a)quinolizin-1-yl)-carbonyl]-2-pyrrolidine-methanol (Ro 19-8022; RO) was kindly provided by F. Hoffmann – LaRoche AG (Basel, Switzerland). Culture media, fetal bovine serum (FBS), antibiotics and other chemicals used for cell cultivation were purchased from GIBCO (Lambda Life, Slovakia). All other chemicals and solvents were of analytical grade from commercial suppliers.

2.2. Inorganic nanoparticles (NPs)

All solid-core inorganic NPs (TiO₂NPs, SiO₂NPs, Fe₃O₄NPs and AuNPs) were synthesized and characterized in-depth by group of Prof. Victor F. Puntes (Institute of Nanoscience and Nanotechnology, Barcelona, Spain). AuNPs were stabilized by sodium citrate (2.2 mM) while dispersant used for TiO₂NPs and Fe₃O₄NPs was TMAOH (tetramethylammonium hydroxide, 10 mM). SiO₂NPs were kept in Milli-Q water. All inorganic NPs were stored in the dark and dry place.

2.3. Dynamic light scattering (DLS)

Particle size distribution and colloidal stability of inorganic NPs in culture medium at 37 °C was determined by DLS using Zetasizer Nano-ZS (Malvern Instruments, UK) equipped with a 4 mW helium/neon laser ($\lambda = 633$ nm) and a thermoelectric temperature controller. The measurements were performed at ~3 min intervals during 1 h at three time intervals – 0 h (0–1 h), 3 h (3–4 h) and 24 h (23–24 h); every data point was recorded as the average of at least 11 repetitions. Instrument set-up was done with respect to the physico-chemical characteristics (absorption, refractive index, viscosity, temperature) of the studied colloidal solutions [16].

2.4. Cell culture

The human renal proximal tubule epithelial TH1 cell line cell line was obtained from Kerfast Inc. (Boston, USA). The cells were cultured in DMEM medium with high glucose supplemented with 10% fetal calf serum (FCS) and antibiotics (penicillin 100 U/ml, streptomycin 100 µg/ml) on plastic Petri dishes (Ø 100 mm) at 37 °C in humidified atmosphere of 5% CO₂.

2.5. Treatment of cells

Exponentially growing cells were exposed to different concentrations of inorganic NPs for 3 h and 24 h. All concentrations were prepared freshly before exposure using procedure provided by Prof. Victor F. Puntes (Institute of Nanoscience and Nanotechnology, Barcelona, Spain) [17]. Briefly, 1 ml of the inorganic NPs was initially mixed with 1 ml of FCS and then culture medium with FCS (9 ml) was added. From this basic stock dispersion of NPs in medium, further dilutions were prepared. The solvents/dispersants (sodium citrate, TMAOH) were also tested for potential cyto- and genotoxic effects. The treatment of the cells was ended by removing the medium with inorganic NPs and washing the cells twice with phosphate-buffered saline (PBS).

2.6. alamarBlue® assay

TH1 cells were seeded into the series of 96 well plates in a density of 2×10^4 /well and cultured in complete culture medium. Exponentially growing cells were then pre-incubated either in the presence of broad range of inorganic NPs, solvents/dispersants or untreated (control) cells for 3 h and 24 h. After treatment, cells were incubated with 100 µl of working solution of alamarBlue® (Invitrogen, USA) for 4 h according to the manufacturer's protocol. The fluorescence (excitation 530 nm, emission 590 nm) in each well was measured on a microplate reader - POLARStar OPTIMA- BMG LABTECH.

2.7. Single-cell gel electrophoresis (SCGE, the comet assay)

The capacity of inorganic NPs to induce DNA strand breaks was analyzed using a medium-throughput format of comet assay (12 minigels *per* slide) according to Shaposhnikov et al. [18] with minor modifications. Briefly, TH1 cells (1.2×10^4) were gently resuspended and mixed in 1% LMP agarose in PBS (Ca²⁺ and Mg²⁺ free); the final concentration of LMP was 0.75%. Twelve drops of 10 µl (one thousand

cells *per drop*) were placed on 1% NMP agarose pre-coated microscopic slides. After solidification of the gels, the slides were placed in lysis solution (2.5 M NaCl, 100 mM Na₂EDTA, 10 mM Tris-HCl, pH = 10 and 1% Triton X-100, at 4 °C) for 1 h to remove cellular proteins. After lysis, slides were transferred to an electrophoresis box and immersed in an alkaline solution (300 mM NaOH, 1 mM Na₂EDTA, pH > 13). After 30 min of unwinding time, a voltage of 25 V (0.7 V/cm) was applied for 20 min at 4 °C. The slides were neutralized with three 5 min washes with Tris-HCl (0.4 M, pH = 7.4) and dried with ethanol. Before scoring, slides were stained with ethidium bromide (EtBr, 5 µg/ml). EtBr-stained nucleoids were examined with Zeiss Axio Imager.Z2 fluorescence microscope (Zeiss, Germany) using the computerized image analysis (Metafer 3.6, MetaSystems GmbH, Altlussheim, Germany). The percentage of DNA in the tail (% of tail DNA) was used as a parameter for DNA damage measurement. One hundred comets were scored *per* each sample in each gel.

2.7.1. Oxidative damage to DNA identified by SCGE (*Fpg*-sensitive sites)

After lysis, slides were washed three times for 5 min in endonuclease buffer (40 mM HEPES-KOH, 0.1 M KCl, 0.5 mM EDTA, pH 8.0) and then incubated with formamidopyrimidine-DNA glycosylase/AP nuclease (*Fpg*, 0.2 U/slide) for 30 min in a humidified atmosphere at 37 °C. The slides were then transferred to an electrophoresis box and immersed in an alkaline solution. SCGE was then performed as described above. The photosensitizer RO 19-8022 was utilized as a positive control in these experiments. The working concentration (1 µM in PBS) was prepared freshly before use. The cells were treated with RO 19-8022 in PBS-G buffer (140 mM NaCl, 3 mM KCl, 8 mM Na₂HPO₄, 1 mM KH₂PO₄, 1 mM CaCl₂, 0.5 mM MgCl₂, 0.1% glucose, pH 7.4) for 2 min, and then the cells were irradiated on ice using a 1000 W halogen lamp (Philips PF811) at a distance of 33 cm for 2 min [19].

2.8. Quantification of the internalized amount of inorganic NPs

Flame atomic absorption spectrometry (FAAS) and inductively coupled plasma mass spectrometry (ICP-MS) were adapted to quantify the cellular uptake of inorganic NPs. Au and Fe contents in cell samples were determined by FAAS (AA240FS, Varian, Australia) after sonication with concentrated nitric acid (Suprapure, Merck, Slovakia). Si and Ti contents in cells were determined by ICP-MS (XSeries 2, Thermo Fisher Scientific, Germany) after sonication and high-pressure microwave digestion with concentrated nitric acid and hydrogen peroxide using standard and collision cell modes, respectively. Sc, Y and In were chosen as internal standards. The detection limits (LODs) of the instruments for Au, Fe, Si, and Ti were 0.010 mg/l; 0.008 mg/l; 0.40 µg/l; and 0.046 µg/l, respectively. The limits of quantification (LOQs) of the instruments for Au, Fe, Si, and Ti were 0.033 mg/l; 0.027 mg/l; 1.3 µg/l; and 0.15 µg/l, respectively.

The cellular uptake of NPs expressed as pg of particular element *per*

cell was finally calculated from the internalized amount of NPs normalized to the total number of treated cells according to the following formula:

$$\text{Internalized amount of NPs per cell} = \frac{\text{internalized amount of NPs}}{\text{number of cells}}$$

2.9. Transmission electron microscopy (TEM)

The uptake and accumulation of inorganic NPs in TH1 cells was evaluated by TEM. Cells were plated on Petri dishes (Ø 60 mm, 3–5 × 10⁵ cells/dish) and exposed to inorganic NPs at exponential phase of growth. After treatment, cells were washed twice with PBS and trypsinized. TH1 cellular suspension (treated with TiO₂NPs, Fe₃O₄NPs, AuNPs or untreated) was centrifuged at 1000 rpm for 5 min in PBS. The samples were then fixed with 4% formaldehyde in PBS for 45 min. After post-fixation with 1% osmium tetroxide (OsO₄) in cacodylate buffer for 30 min, samples were contrasted overnight with a saturated aqueous solution of uranyl acetate at room temperature. The samples were then dehydrated in graded ethanol series and propylene oxide, and embedded into Durcupan (Fluka AG, Switzerland). Ultrathin (60 nm) sections were cut by Power-Tome MT-XL (RMC/Sorvall, Tucson, USA) ultramicrotome, placed on copper grids covered with formvar membranes and contrasted by lead citrate. The sections were examined with JEM 1200 electron microscope (Jeol, Tokyo, Japan) at 7500–50000 × magnification. Images were recorded using a Gatan Dual Vision 300 W CCD camera (Gatan Inc., Pleasanton, USA).

2.10. Statistical analysis

Data are given as mean values with ± SD. The differences between control cells and treated cells were evaluated by Student's *t*-test and one-way analysis of variance (ANOVA). The threshold of statistical significance was set to *p* < 0.05.

3. Results

3.1. Characteristics of inorganic NPs, particle size distribution and colloidal stability in culture medium

As physico-chemical properties of NPs are critical to understand their biological activity, prior to nanotoxicity testing, the characterization of concentration, particle size and ζ-potential of tested NPs has been performed. The basic physico-chemical characteristics of tested inorganic NPs after preparation are summarized in Table 1. Except SiO₂NPs, the core size of all tested NPs was nearly identical.

The particle size distribution and colloidal stability of particular NPs in culture medium was measured at three concentrations (Table 2). The hydrodynamic particle size of each type of NPs increased substantially in DMEM medium due to agglomeration of particles and absorption of

Table 1
Basic physico-chemical properties of tested inorganic NPs.


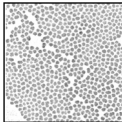
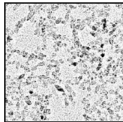
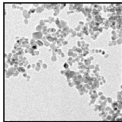
Nanoparticles	AuNPs	SiO ₂ NPs	TiO ₂ NPs	Fe ₃ O ₄ NPs
inner core diameter [nm]	13.8 ± 1.71	27.6 ± 3.8	5 – 10	7-15
Particle size (DH) diameter in solvent [nm]	13.8 ± 0.58 (sodium citrate, 2.2 mM)	30.19 ± 10.65 (Mili-Q water)	23.67 ± 7.93 (tetramethylammonium hydroxide, 10 mM)	19.12 ± 3.91 (tetramethylammonium hydroxide, 10 mM)
PDI	0.219 ± 0.29	0.217 ± 0.01	0.174 ± 0.005	0.437 ± 0.038
Zeta (ξ) potential [mV]	-40.9 ± 2.76	-52.1 ± 10.4	-42.0 ± 15.4	-35.9 ± 3.87
Concentration in stock [mg/ml]	0.066	10.15	5	11.6
Number of particles/ml	~3.02 × 10 ¹²	~3 × 10 ¹⁴	~5 × 10 ¹⁵	~5 × 10 ¹⁵
TEM image				

Table 2
Size distribution of TiO₂NPs, SiO₂NPs, Fe₃O₄NPs and AuNPs in culture medium.

TiO ₂ NPs									
	0 h	165 µg/ml		0 h	22 µg/ml		0 h	2.2 µg/ml	
		3 h	24 h		3 h	24 h		3 h	24 h
PdI	0.32 ± 0.03	0.32 ± 0.03	0.29 ± 0.01	0.53 ± 0.06	0.46 ± 0.04	0.39 ± 0.06	0.71 ± 0.18	0.42 ± 0.08	0.26 ± 0.01
Z-Ave	251 ± 5	251 ± 5	251 ± 5	204 ± 11	223 ± 4	234 ± 11	161 ± 45	238 ± 10	231 ± 5
Size [nm] (Number)	83 ± 42	72 ± 47	83 ± 45	88 ± 61	91 ± 57	81 ± 53	89 ± 47	80 ± 61	120 ± 38
Size [nm] (Intensity)	367 ± 17	368 ± 26	350 ± 21	357 ± 26	365 ± 29	356 ± 14	357 ± 37	376 ± 22	310 ± 14
Intensity peaks	367 ± 17	368 ± 26	350 ± 21	6 ± 1; 356 ± 24	6 ± 1; 365 ± 29	356 ± 14	6 ± 1; 357 ± 37	376 ± 22	310 ± 14
SiO ₂ NPs									
	0 h	165 µg/ml		0 h	22 µg/ml		0 h	2.2 µg/ml	
		3 h	24 h		3 h	24 h		3 h	24 h
PdI	0.56 ± 0.10	0.26 ± 0.01	0.19 ± 0.01	0.53 ± 0.20	0.27 ± 0.02	0.22 ± 0.01	0.55 ± 0.14	0.30 ± 0.06	0.17 ± 0.01
Z-Ave	68 ± 20	130 ± 3	148 ± 2	83 ± 22	132 ± 1	140 ± 2	58 ± 29	124 ± 6	146 ± 2
Size [nm] (Number)	6 ± 1*	87 ± 9	111 ± 6	6 ± 1*	94 ± 8	102 ± 8	6 ± 1*	93 ± 9	110 ± 5
Size [nm] (Intensity)	143 ± 17	174 ± 4	179 ± 4	153 ± 22	178 ± 7	176 ± 4	141 ± 51	174 ± 5	174 ± 4
Intensity peaks	143 ± 17	174 ± 4	179 ± 4	24 ± 4; 153 ± 22	178 ± 7	176 ± 4	141 ± 51	174 ± 5	174 ± 4
Fe ₃ O ₄ NPs									
	0 h	165 µg/ml		0 h	22 µg/ml		0 h	2.2 µg/ml	
		3 h	24 h		3 h	24 h		3 h	24 h
PdI	0.40 ± 0.10	0.43 ± 0.08	0.28 ± 0.01	0.61 ± 0.15	0.54 ± 0.08	0.38 ± 0.006	0.53 ± 0.15	0.46 ± 0.07	0.28 ± 0.01
Z-Ave	720 ± 27	617 ± 16	355 ± 4	485 ± 70	415 ± 28	180 ± 6	166 ± 63	174 ± 21	145 ± 1
Size [nm] (Number)	495 ± 302	317 ± 188	222 ± 87	20 ± 33	127 ± 89	66 ± 54	7 ± 0.6*	62 ± 30	110 ± 10
Size [nm] (Intensity)	973 ± 281	921 ± 196	488 ± 18	628 ± 61	671 ± 184	275 ± 16	390 ± 112	250 ± 15	197 ± 4
AuNPs									
	0 h	2.2 µg/ml		0 h	0.66 µg/ml		0 h	0.22 µg/ml	
		3 h	24 h		3 h	24 h		3 h	24 h
PdI	0.36 ± 0.03	0.67 ± 0.07	0.29 ± 0.01	0.45 ± 0.13	0.62 ± 0.09	0.33 ± 0.01	0.59 ± 0.28	0.40 ± 0.09	0.27 ± 0.01
Z-Ave	17 ± 1	52 ± 15	139 ± 2	18 ± 10	87 ± 12	126 ± 2	56 ± 36	119 ± 8	136 ± 2
Size [nm] (Number)	6 ± 0.3*	6 ± 1*	124 ± 7	6 ± 1*	6 ± 0.4*	117 ± 8	6 ± 1*	7 ± 1*	111 ± 7
Size [nm] (Intensity)	26 ± 11	173 ± 26	192 ± 3	23 ± 13	183 ± 10	185 ± 4	127 ± 64	190 ± 3	182 ± 3
Intensity peaks	12 ± 2; 59 ± 14	6 ± 1; 190 ± 4	7 ± 1; 198 ± 4	8 ± 1; 58 ± 11	8 ± 1; 198 ± 3	185 ± 6	7 ± 1; 58 ± 12	7 ± 1; 196 ± 6	183 ± 5

* Particles from serum proteins, probably BSA.

serum protein(s) on particle surface (protein corona formation). Fe₃O₄NPs that manifested polydisperse distribution were colloiddally unstable at 165 and 22 µg/ml concentrations and their aggregation and sedimentation were visible already after visual inspection. At the lowest 2.2 µg/ml concentration, the colloid dispersion was relatively stable within the tested time frame. All other types of NPs: AuNPs, TiO₂NPs and SiO₂NPs were colloiddally stable in culture medium at all three concentrations used. At the low concentrations (≤ 2.2 µg/ml), DLS measurements were strongly affected by the presence of small particles representing the serum proteins (probably BSA) as they are in high excess in culture medium in comparison to inorganic NPs. In line with Ji et al. [20], DLS analysis of NPs-free medium (DMEM + 10% FBS + ATB) confirmed the presence of 6 ± 1 nm particles.

3.2. Cytotoxicity

A broad range of concentrations of particular inorganic NPs was utilized to evaluate their effect on viability of TH1 cells. In order to cover as wide concentration range as possible for the cytotoxicity testing, the highest concentration of particular NP has been calculated based upon the stock concentration (see Material and Methods), hence the differences between tested NPs. Concentrations ranging from 0.1 to 3 µg/ml (AuNPs); from 6 to 924 µg/ml (SiO₂NPs), from 58 to 1056 µg/ml (Fe₃O₄NPs); and from 83 to 454 µg/ml (TiO₂NPs) were applied to

TH1 cells for 3 h and 24 h. Under these treatment conditions, none of the tested inorganic NPs, except Fe₃O₄NPs at higher concentrations (> 700 µg/ml), manifested any cytotoxic effects either after 3 h or 24 h (Fig. 1A–D). No cytotoxic effect was determined after treatment of TH1 cells with the highest concentration of particular solvents/dispersants after 24 h (data not shown).

3.3. Genotoxicity

Based on the recommendation of EU-funded NaNoReg and NanoTest projects [21], the concentrations 2.2, 22, and 165 µg/ml (corresponding to 1, 10 and 75 µg/cm²) were selected for SiO₂NPs, TiO₂NPs and Fe₃O₄NPs. None of these concentrations had any cytotoxic effect as shown earlier (Fig. 1A–D). In the case of AuNPs, the concentrations 0.22, 0.66 and 2.2 µg/ml (corresponding to 0.1, 0.3 and 1 µg/cm²) were used as the concentration of stock solution was substantially lower. The impact of inorganic NPs on genome stability was determined by the alkaline comet assay. In order to simulate more realistic *in vivo* kidney conditions, TH1 cells were seeded on Transwell polycarbonate membrane cell culture inserts (3 µm pore density) and exposed to inorganic NPs under static and dynamic conditions for 3 h and 24 h. Medium flow rate - 20 µl/min, corresponded in our experimental setup to ~ 0.2 dyn/cm⁻² which reflects the *in vivo* situation in kidneys according to Ingber et al. [22]. In addition to DNA breakage,

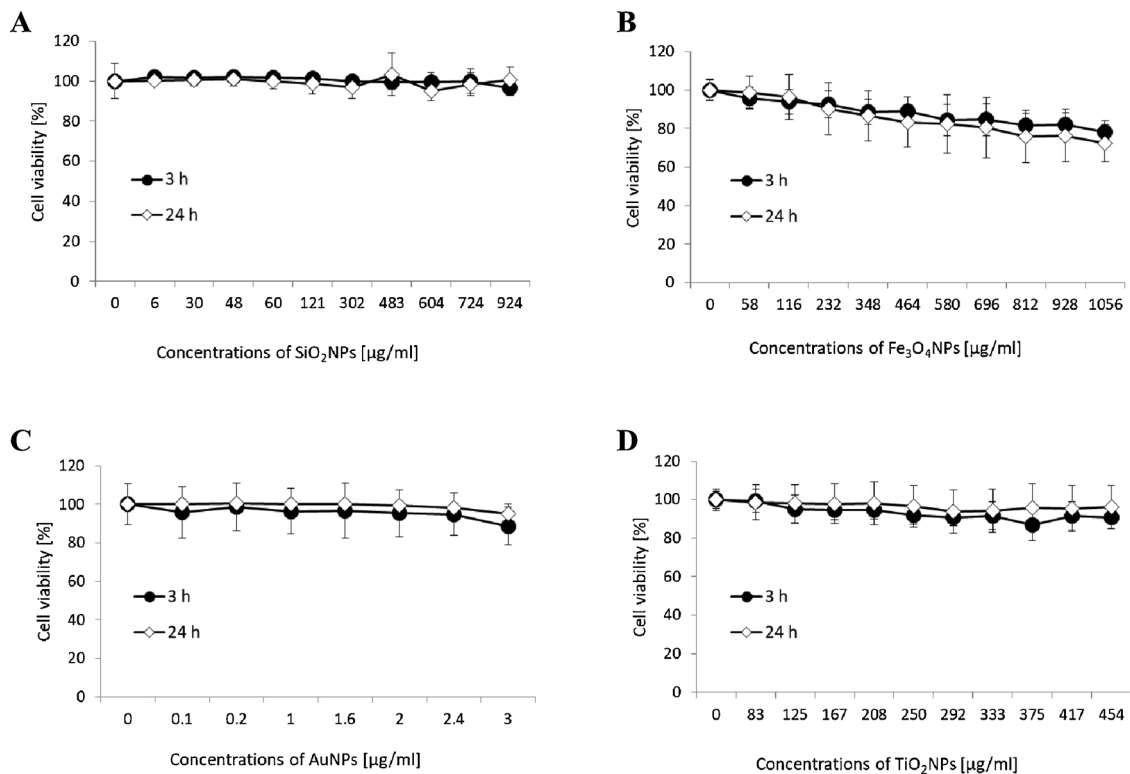


Fig. 1. Cell viability of TH1 cells treated with inorganic NPs.

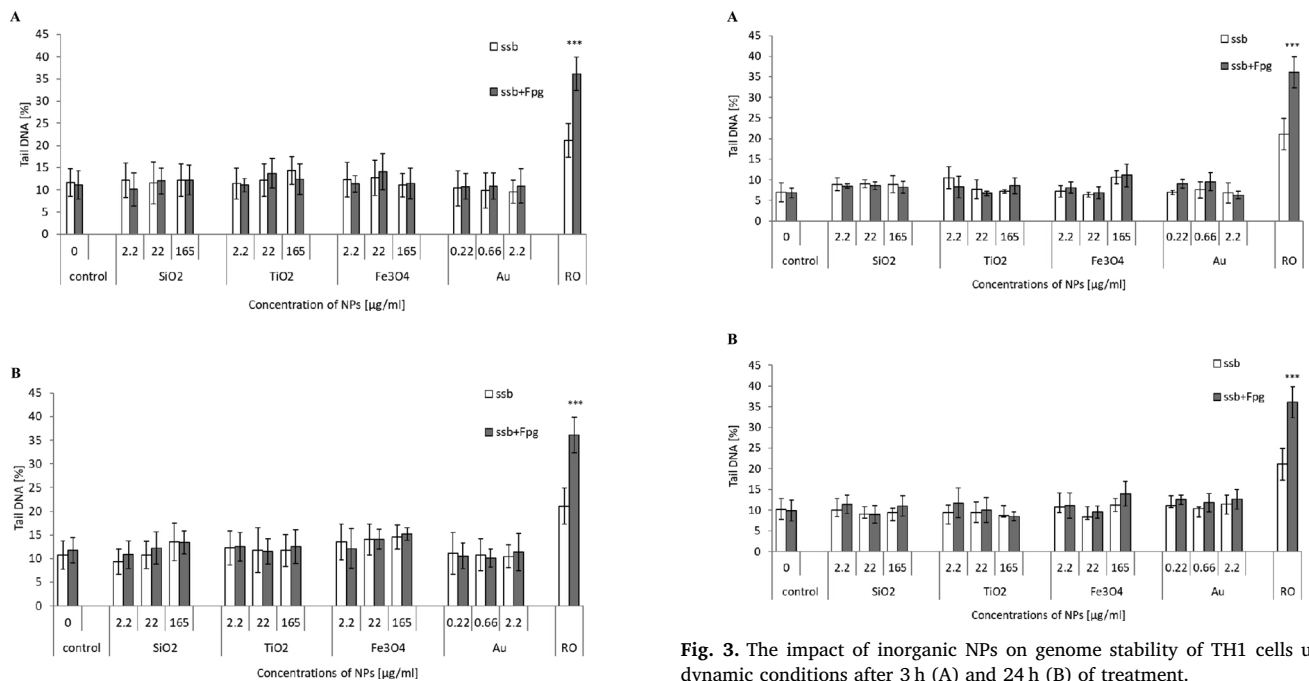


Fig. 2. The impact of inorganic NPs on genome stability of TH1 cells under static conditions after 3 h (A) and 24 h (B) of treatment.

the capacity of inorganic NPs to induce oxidative DNA damage was assessed as well. None of the inorganic NPs increased significantly the level of DNA strand breaks and oxidative DNA damage in TH1 cells compared to control cells when treated under static conditions (Fig. 2A and B). Similar results were obtained when TH1 cell were treated with inorganic NPs under dynamic conditions. No significant increase in the level of DNA strand breaks and oxidative damage to DNA were determined (Fig. 3A and B). Also no changes in basal level of DNA damage

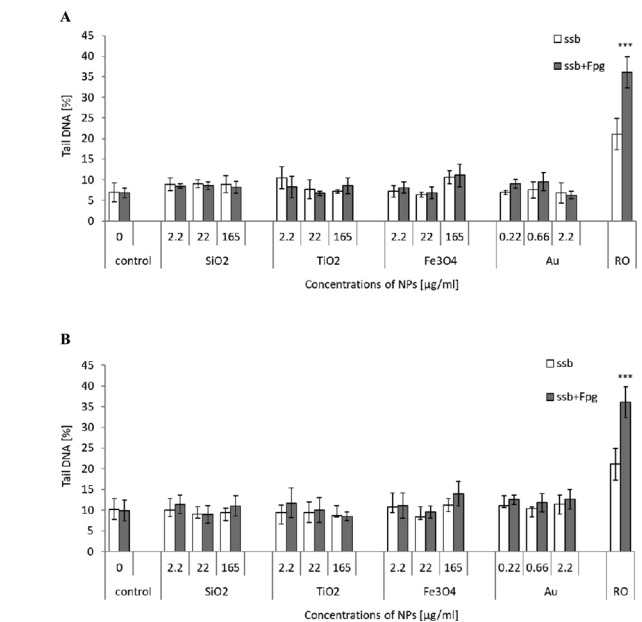


Fig. 3. The impact of inorganic NPs on genome stability of TH1 cells under dynamic conditions after 3 h (A) and 24 h (B) of treatment.

in control TH1 cells were observed upon dynamic exposure [$6.98\% \pm 2.36\%$ (3 h) or $10.13\% \pm 2.67\%$ (24 h)] when compared to static conditions $11.63\% \pm 3.15\%$ (3 h) or $10.79\% \pm 2.97\%$ (24 h).

3.4. Quantification of internalized NPs

For the nanosafety assessment, the quantification of internalized amount of NPs is critical step and supports the association between the amount of internalized nanoparticles and their biological effect. In order to explain the absence of any impact on cell viability and the level

Table 3

The amount of elements (Ti, Si, Fe and Au) detected in TH1 cells exposed to TiO₂NPs, SiO₂NPs, Fe₃O₄NPs (2.2 µg/ml, 24 h) and the uptake efficiency in TH1 cells. The amount of particular element [pg/cell] is expressed as the net value.

	Ti [pg/cell]	Si [pg/cell]	Fe [pg/cell]	Au [pg/cell]	Cell number [x10 ⁶]	Total applied dose [µg]	Internalized amount	
							Total [µg]	[%] from total applied dose
Control cells	0.0018	0.0991	0.0228	0.0	13.20	–	–	–
TiO ₂ NPs	0.0107	–	–	–	10.25	33.0	0.128	0.389
SiO ₂ NPs	–	0.0430	–	–	8.90	33.0	1.265	3.833
Fe ₃ O ₄ NPs	–	–	1.4672	–	8.83	33.0	13.190	39.970
AuNPs	–	–	–	0.8652	7.42	33.0	6.420	19.455

of DNA damage (strand breaks and oxidative DNA damage), the FAAS and ICP-MS were employed to rule out the possibility of the failure of studied NPs to enter the cells. Additionally, to compare the efficacy of NPs uptake based on their chemical composition, exponentially growing TH1 cells were exposed to equivalent concentration (2.2 µg/ml) of the tested inorganic NPs for 24 h. The basal level of particular elements (Fe, Si, Ti and Au) was determined also in control (untreated) cells to avoid any false positive results. The Table 3 summarizes the internalized amount of different elements (expressed as pg of Ti, Si, Fe, or Au per cell).

As small amounts of Ti, Si and Fe were detected also in control (untreated) TH1, these quantities were subtracted from the total amounts of particular elements detected in exposed cells, and the data presented in the Table 3 represent the net quantity. Taking into the account the initial amount of NPs that has been used to treat TH1 cell, the efficacy of the uptake has been calculated and showed that TH1 cells internalized more efficiently Fe₃O₄NPs and AuNPs compared to SiO₂NPs and TiO₂NPs. As the hydrodynamic size of all inorganic NPs in culture medium was nearly the same (110–120 nm agglomerates) the effect of chemical composition on NPs uptake cannot be excluded. Moreover, the core size of inorganic NPs was nearly identical except SiO₂NPs (Table 1).

3.5. The accumulation of NPs in TH1 cells

Following the 24 h treatment with equivalent concentration (2.2 µg/ml TiO₂NPs, Fe₃O₄NPs and AuNPs), TH1 cells were processed for electron microscopy to study the impact of inorganic NPs on their ultrastructure, preferential accumulation inside the cells and possible mechanism of internalization. The electron microscopy analysis revealed that all the tested NPs (regardless on the chemical composition) are present inside the TH1 cells as of vesicles containing NPs were observed in cytoplasm (Fig. 4A–C). Based on the observation performed with cells exposed to 165 µg/ml Fe₃O₄NPs, it is reasonable to predict that the inorganic NPs are internalized by a process similar to phagocytosis that manifested at the active surface of the cell (Fig. 5A–B). The small aggregates of NPs at the cell surface were surrounded by the protrusions of plasma membrane and engulfed in vesicles to the cell (Fig. 5B–D). Phagosomes with NPs interact with lysosomes and form

phagolysosomes. The size of the phagolysosomes and their occurrence in the cytosol of the cells varied. The occasionally observed fusion of phagolysosomes (Fig. 5C), may explain the presence of large phagolysosomes filled with accumulated NPs (Fig. 5D). Phagolysosomes contained nanoparticles in dense condensed form together with the grain matter (Fig. 5A–C). Lipofuscin granules and autophagosomes (Fig. 5D) were rarely present. These observations indicate that TH1 cells cannot process excess of NPs, for instance by exocytosis or encapsulation, since these processes were not observed. An excessive accumulation of NPs destroys the structure of cells to the extent that prevents their normal function and, in effect, may lead to cell inactivity, death and formation of tissue scars.

4. Discussion

Renal clearance of nanoparticles, which have reached the systemic circulation, is an expected and possible elimination route in living organisms. For this reason, kidneys might be one of the most important secondary target organs; and the NPs-induced renal toxicity should be carefully evaluated.

Several *in vitro* and *in vivo* studies have reported that different types of NPs are able to exert various toxic effects in renal cells/tissue [5], however the number of such studies is limited. Additionally, because of the diversity of NPs, especially their physico-chemical properties that influence their characteristics and behavior, many nano-bio interactions still remain to be understood. Therefore, to provide a comprehensive and critical evaluation of the toxicity of NPs on the renal system further studies are inevitable. The employment of cell culture techniques in (nano)toxicology has gained more importance over the past decades in order to minimize the experiments on animals. Cowie et al. [23] studied the suitability of mammalian cells of different origin for the assessment of genotoxicity of various NPs and the kidney cells used in their study (HEK293 and COS1) seemed to be one of the most reliable to detect a dose-response upon NPs treatment. The currently available and used *in vitro* human renal cell models such as HK-2 cells and HEK293 cells (reviewed in [24], this Special Issue), however, lack sufficient *in vivo* physiological relevance as the cells are in the majority of studies cultivated under static conditions as two dimensional (2D) cultures.

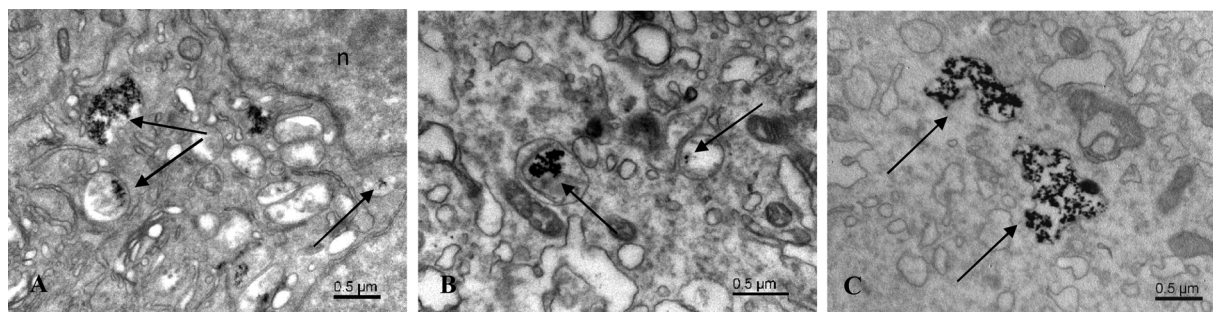


Fig. 4. Accumulation of NPs in the TH1 cells treated with 2.2 µg/ml TiO₂NPs, AuNPs, and Fe₃O₄NPs for 24h.

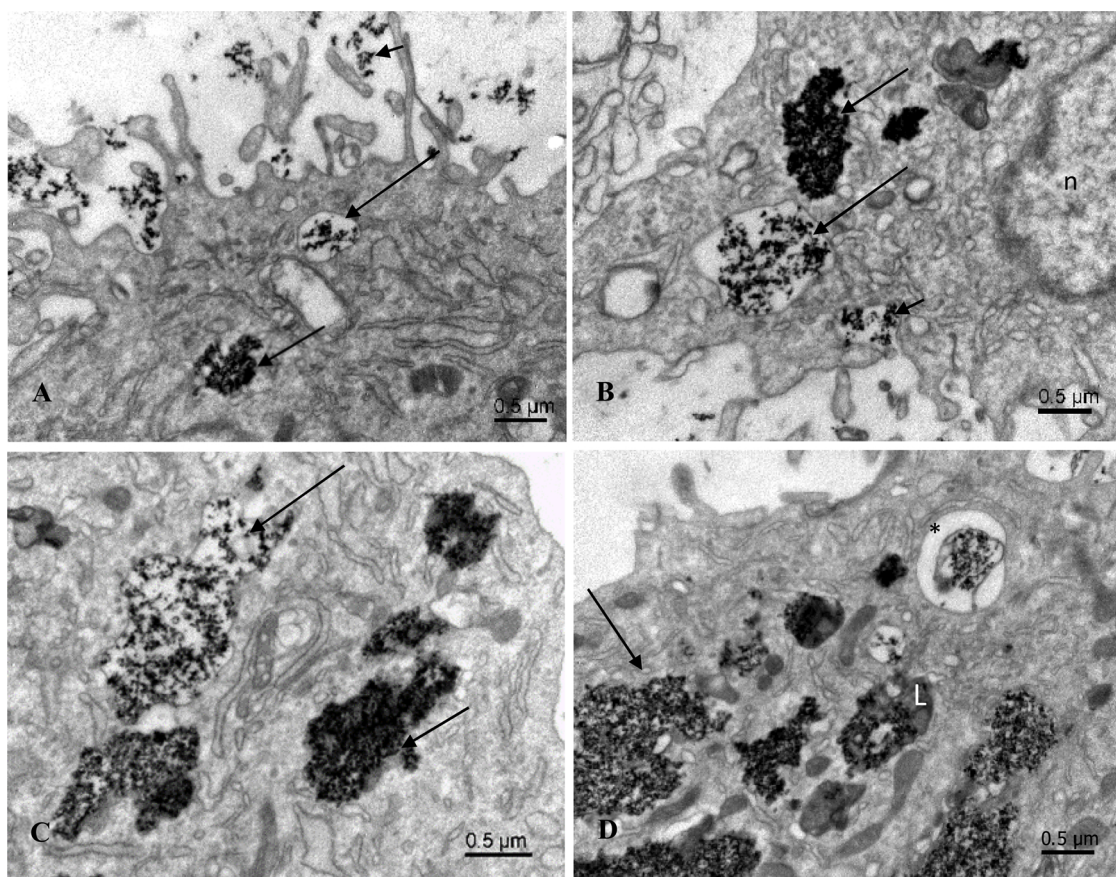


Fig. 5. Electron-microscopic images of ultrastructure TH1 cells exposed to 165 µg/ml $\text{Fe}_3\text{O}_4\text{NPs}$ for 24 h.

In order to evaluate the impact of selected inorganic NPs under more realistic *in vivo* conditions, the human renal TH1 cells were grown in this study on Transwell membrane inserts and treated with inorganic NPs under continuous medium flow rate. It has been suggested that combination of *in vitro* methods simulating as closely as possible *in vivo* conditions should be used to access the possible toxic effects of NPs [25]. Moreover, culturing TH1 cells on permeable supports also promotes apical-basal polarization that is an important characteristic of mature epithelial layers, thereby simulating *in vivo* conditions.

Four inorganic solid-core NPs (TiO_2NPs , SiO_2NPs , $\text{Fe}_3\text{O}_4\text{NPs}$ and AuNPs) that can be found in everyday life commercial products were evaluated in this study. All inorganic NPs except $\text{Fe}_3\text{O}_4\text{NPs}$ at higher concentrations were colloiddally stable in culture medium during 24 h, though the particle size of individual NPs increased substantially probably due to particle agglomeration and protein corona formation [26,27]. None of the inorganic NPs induced any DNA strand breaks and oxidative DNA lesions regardless of the exposure (static and dynamic conditions). Even with the use of unrealistically high concentrations (with respect to the common human exposure), no cytotoxicity was observed, with the exception of $\text{Fe}_3\text{O}_4\text{NPs}$ ($> 700 \mu\text{g/ml}$). Despite the fact that the surface coating of NPs is a widely used procedure to increase the biocompatibility and reduce the potential toxicity, there are also studies [28] showing no (or low) cytotoxic effect of uncoated inorganic NPs (*etc.* $\text{Fe}_3\text{O}_4\text{NPs}$) which is in agreement with our findings. Moreover, our results were in line with L'Azou et al. [14], Halamoda Kenzaoui et al. [11] and Kermanizadeh et al. [29] who did not detect any significant increase in ROS formation in human or mammalian renal cells after exposure to TiO_2NPs , $\text{Fe}_3\text{O}_4\text{NPs}$ and SiO_2NPs . On the other hand, intracellular ROS generation was detected in human renal HK-2, HEK293 cells and human mesangial IP15 cells [7,30,31], porcine renal LLC-PK1 cells [32], and rat kidney proximal tubular NRK-52E

cells [33] after exposure to inorganic NPs (AuNPs , TiO_2NPs , ZnONPs , SiO_2NPs , CdNPs , AgNPs). Oxidative stress and generation of reactive oxygen species (ROS) has been proposed as one of the main mechanisms underlying NP-induced toxicity [34]. ROS formation may occur due to NP-mediated damage to the mitochondrial membrane [35] or NPs may affect the NADPH oxidase in the plasma membrane during entry into the cell [36]. In the case of iron oxide NPs, it is supposed that iron ions released from the particle surface due to lysosomal enzymatic degradation can participate in the Fenton reaction, producing the hydroxyl radicals [37]. Treatment of HEK293 cells with $\text{Fe}_2\text{O}_3\text{NP}$ -conditioned medium revealed that the cytotoxic effect induced by $\text{Fe}_2\text{O}_3\text{NPs}$ *per se* was much higher so the authors concluded that the contribution of metal ion release to $\text{Fe}_2\text{O}_3\text{NPs}$ cytotoxicity was fairly low [38].

The glomerular filtration apparatus possesses an effective size cutoff of 10 nm, in case of metal-based NPs the threshold of 5.5 nm was defined by investigation of the renal clearance of quantum dots of different sizes [39]. In contrast to glomerular filtration membrane, which acts as a physical barrier (size and charge barrier), the proximal tubules behave as a chemical barrier for NPs because of their active endocytic machinery. After glomerular filtration, nanoparticles are concentrated in the proximal tubules, which can lead to internalization by tubular cells through endocytosis [40]. However, despite the size cutoff, it has been shown by Zuckerman et al. [41] that polycationic cyclodextrin NPs containing siRNA ($\sim 70 \text{ nm}$) accumulated in glomerular mesangium and Williams et al. [42] reported that the "mesoscale" nanoparticles (PLGA-PEG, 400 nm, i.v. administration) localized selectively in renal proximal tubules. Also study by Oroojalian et al. [43] showed that modified-polymyxin-PEI/DNA nanoparticles can effectively target megalin-expressing kidney cells (megalin being one of the markers for proximal tubule cells). Taking into consideration the physico-chemical properties (especially size), all the tested inorganic NPs represent non-

renal clearable NPs that would be unable to pass glomerular filtration. However, the full potential to induce any nephrotoxic changes *in vivo* is difficult to predict.

Although no cyto- or genotoxic effects were determined in TH1 cells after 3 h or 24 h treatment, TEM and FAAS analyses clearly demonstrated that all inorganic NPs tested in this study are internalized as agglomerates into the cells probably due to extremely dynamic endocytic machinery that is the characteristic feature of the renal proximal tubules. Inorganic NPs localized in vesicles surrounded by the plasma membrane were accumulated in cytoplasm. Occasionally, these NP-filled vesicles fused with lysosomes creating phagolysosomes. This phenomenon indicated that TH1 cells cannot process excess of NPs, for instance by exocytosis or encapsulation as these processes were not observed. Substantial differences in the internalized amount of particular inorganic NPs determined in TH1 cells exposed to equivalent concentration of NPs indicate that the physico-chemical characteristics affect the efficacy of the uptake. As summarized by Oh and Park [44], it is believed that the endocytosis efficiency of NPs is strongly dependent on their properties, such as size, shape, and surface chemistry, as well as cell type and our previous studies confirmed it as well [45].

In summary, TH1 cells were exposed to inorganic NPs under continuous medium flow rate to mimic more realistic the *in vivo* conditions. Although the inorganic NPs were internalized into TH1 cells, none of them induced any profound cyto- and genotoxic effects. The comet assay, also called single cell gel electrophoresis (SCGE), is a sensitive and rapid technique for quantifying and analyzing DNA damage in individual cells. This method was adopted for fast screening of genetic changes to DNA induced by NPs [46]. The medium throughput comet assay method used in this study allowed not only the acceleration of the NPs-induced nephrotoxicity screening but additionally minimized the influence of confounding factor on results as all slides (with and without restriction enzyme incubation) were processed under the same experimental conditions.

Conflict of interest

The authors declare that there are no conflicts of interests.

Acknowledgements

The authors would like to thank to Prof. Victor F. Puntes (Institute of Nanoscience and Nanotechnology, Barcelona, Spain) who kindly provided inorganic nanoparticles and Ladislav Novota from Institute of Experimental Endocrinology BMC SAS, Department of Cellular Cardiology for technical assistance with EM experiments.

This article was created by the realization of the H2020 project HISENTS No. 685817, COST Action CA15132, VEGA grant 2/0056/17, project "Center of excellence of environmental health", ITMS No. 26240120033, based on the support of operational Research and development program financed from the European Regional Development Fund; and the EEA projectSK0020. Filip Razga received support within the SASPRO Programme (Project No. 0057/01/02) co-funded by the European Union and the Slovak Academy of Sciences.

References

- [1] E.A. Lock, C.J. Reed, Xenobiotic metabolizing enzymes of the kidney, *Toxicol. Pathol.* 26 (1998) 18–25.
- [2] J.W. Lohr, G.R. Willsky, M. a Acara, Renal drug metabolism, *Pharmacol. Rev.* 50 (1998) 107–141 <https://doi.org/10.1177/019262339802600102>.
- [3] T. Wu, M. Tang, Review of the effects of manufactured nanoparticles on mammalian target organs, *J. Appl. Toxicol.* 38 (2018) 25–40, <https://doi.org/10.1002/jat.3499>.
- [4] R. Landsiedel, U.G. Sauer, L. Ma-Hock, J. Schnekenburger, M. Wiemann, Pulmonary toxicity of nanomaterials: a critical comparison of published *in vitro* assays and *in vivo* inhalation or instillation studies, *Nanomedicine* 9 (2014) 2557–2585, <https://doi.org/10.2217/nmm.14.149>.
- [5] I. Iavicoli, L. Fontana, G. Nordberg, The effects of nanoparticles on the renal system, *Crit. Rev. Toxicol.* 46 (2016) 490–560, <https://doi.org/10.1080/10408444.2016.1181047>.
- [6] Z. Chen, H. Meng, G. Xing, C. Chen, Y. Zhao, G. Jia, T. Wang, H. Yuan, C. Ye, F. Zhao, Z. Chai, C. Zhu, X. Fang, B. Ma, L. Wan, Acute toxicological effects of copper nanoparticles *in vivo*, *Toxicol. Lett.* 163 (2006) 109–120, <https://doi.org/10.1016/j.toxlet.2005.10.003>.
- [7] F. Wang, F. Gao, M. Lan, H. Yuan, Y. Huang, J. Liu, Oxidative stress contributes to silica nanoparticle-induced cytotoxicity in human embryonic kidney cells, *Toxicol. In Vitro* 23 (2009) 808–815, <https://doi.org/10.1016/j.tiv.2009.04.009>.
- [8] J. Chen, X. Dong, J. Zhao, G. Tang, *In vivo* acute toxicity of titanium dioxide nanoparticles to mice after intraperitoneal injection, *J. Appl. Toxicol.* 29 (2009) 330–337, <https://doi.org/10.1002/jat.1414>.
- [9] Y. Yamagishi, A. Watari, Y. Hayata, X. Li, M. Kondoh, Y. Yoshioka, Y. Tsutsumi, K. Yagi, Acute and chronic nephrotoxicity of platinum nanoparticles in mice, *Nanoscale Res. Lett.* 8 (2013) 1–7, <https://doi.org/10.1186/1556-276X-8-395>.
- [10] C. Ashajyothi, H.K. Handral, C.R. Kelmani, A comparative *in vivo* scrutiny of bio-synthesized copper and zinc oxide nanoparticles by Intraperitoneal and intravenous administration routes in rats, *Nanoscale Res. Lett.* 13 (2018) 93, <https://doi.org/10.1186/s11671-018-2497-2>.
- [11] B. Halamoda Kenzaoui, C. Chapuis Bernasconi, L. Juillerat-Jeanerret, Stress reaction of kidney epithelial cells to inorganic solid-core nanoparticles, *Cell Biol. Toxicol.* 29 (2013) 39–58, <https://doi.org/10.1007/s10565-012-9236-8>.
- [12] J. Wang, G. Zhou, C. Chen, H. Yu, T. Wang, Y. Ma, G. Jia, Y. Gao, B. Li, J. Sun, Y. Li, F. Jiao, Y. Zhao, Z. Chai, Acute toxicity and biodistribution of different sized titanium dioxide particles in mice after oral administration, *Toxicol. Lett.* 168 (2007) 176–185, <https://doi.org/10.1016/j.toxlet.2006.12.001>.
- [13] M.A.K. Abdelhalim, B.M. Jarrar, Renal tissue alterations were size-dependent with smaller ones induced more effects and related with time exposure of gold nanoparticles, *Lipids Health Dis.* 10 (2011), <https://doi.org/10.1186/1476-511X-10-163>.
- [14] B. L'Azou, J. Jorly, D. On, E. Sellier, F. Moisan, J. Fleury-Feith, J. Cambar, P. Brochard, C. Ohayon-Courtes, *In vitro* effects of nanoparticles on renal cells, *Part. Fibre Toxicol.* 5 (2008) 1–14, <https://doi.org/10.1186/1743-8977-5-22>.
- [15] C.M. Kowolik, S. Liang, Y. Yu, J.-K. Yee, Cre-mediated reversible immortalization of human renal proximal tubular epithelial cells, *Oncogene* 23 (2004) 5950–5957, <https://doi.org/10.1038/sj.onc.1207801>.
- [16] V. Némethová, B. Buliaková, P. Mazancová, A. Bábelová, Š. Michal, D. Morav, L. Kle, M. Ursínyová, A. Gábelová, F. Rázga, Intracellular uptake of magnetite nanoparticles: a focus on physico-chemical characterization and interpretation of *in vitro* data, *Mater. Sci. Eng. C* 70 (2017) 161–168, <https://doi.org/10.1016/j.msec.2016.08.064>.
- [17] G.J. Oostingh, E. Casals, P. Italiani, R. Colognato, R. Stritzinger, J. Ponti, T. Pfaller, Y. Kohl, D. Ooms, F. Favilli, H. Leppens, D. Lucchesi, F. Rossi, I. Nelissen, H. Thielecke, V.F. Puntes, A. Duschl, D. Boraschi, Problems and challenges in the development and validation of human cell-based assays to determine nanoparticle-induced immunomodulatory effects, *Part. Fibre Toxicol.* (2011) 1–21.
- [18] S. Shaposhnikov, A. Azqueta, S. Henriksson, S. Meier, I. Gaivão, N.H. Huskisson, A. Smart, G. Brunborg, M. Nilsson, A.R. Collins, Twelve-gel slide format optimised for comet assay and fluorescent *in situ* hybridisation, *Toxicol. Lett.* 195 (2010) 31–34, <https://doi.org/10.1016/j.toxlet.2010.02.017>.
- [19] A. Collins, C. Gedik, N. Vaughan, S. Wood, A. White, J. Dubois, J.F. Rees, S. Loft, P. Møller, H. Poulsen, J. Cadet, T. Douki, J.L. Ravanat, S. Sauvaigo, H. Faure, I. Morel, B. Morin, B. Epe, N. Phoa, A. Hartwig, T. Schwerdtle, P. Dolara, L. Giovannelli, M. Lodovici, R. Olinski, K. Bialkowski, M. Fokinski, D. Gackowski, Z. Duračková, L. Hlinčíková, P. Korytar, M. Sivanová, M. Dušinská, C. Mislanová, J. Viña, L. Möller, T. Hofer, J. Nygren, E. Gremaud, K. Herbert, J. Lunec, C. Wild, L. Hardie, J. Olliver, E. Smith, Measurement of DNA oxidation in human cells by chromatographic and enzymic methods, *Free Radic. Biol. Med.* 34 (2003) 1089–1099, [https://doi.org/10.1016/S0891-5849\(03\)00041-8](https://doi.org/10.1016/S0891-5849(03)00041-8).
- [20] Z. Ji, E. Suarez, X. Wang, H. Meng, X. Tian, G. Saji, X. Jin, H. Zhang, E.M.V. Hoek, H. Godwin, A.E. Nel, Dispersion and stability optimization of TiO₂ nanoparticles in cell culture media, *Environ. Sci. Technol.* 44 (2014) 7309–7314, <https://doi.org/10.1021/es100417s.Dispersion>.
- [21] M. Dusinska, N. El Yamani, A.R. Collins, E. Rundén-Pran, L.M. Fjellsbo, S. Shaposhnikov, S. Zienolddiny, *In vitro* genotoxicity testing of four reference metal nanomaterials, titanium dioxide, zinc oxide, cerium oxide and silver: towards reliable hazard assessment, *Mutagenesis* 32 (2017) 117–126, <https://doi.org/10.1093/mutage/gew060>.
- [22] D.E. Ingber, Human kidney proximal tubule on a chip for drug transport and nephrotoxicity assessment, *Integr. Biol. (Camb.)* 5 (2013) 1089–1198, <https://doi.org/10.1039/c3ib40049b>.
- [23] H. Cowie, Z. Magdolenova, M. Saunders, M. Drlickova, S. Correia Carreira, B. Halamoda Kenzaoui, L. Gombau, R. Guadagnini, Y. Lorenzo, L. Walker, L.M. Fjellsbo, A. Huk, A. Rinna, L. Tran, K. Volkovova, S. Boland, L. Juillerat-Jeanerret, F. Marano, A.R. Collins, M. Dusinska, Suitability of human and mammalian cells of different origin for the assessment of genotoxicity of metal and polymeric engineered nanoparticles, *Nanotoxicology* 9 (2015) 57–65, <https://doi.org/10.3109/17435390.2014.940407>.
- [24] A. Gabelova, K. Kozics, L. Kapka-Skrzypczak, M. Kruszewski, M. Sramkova, Nephrotoxicity: topical issue, *Mut. Res. Gen. Tox. Environ. Mutagen* (2018) Special Issue 2018, accepted.
- [25] A.R. Collins, B. Annangi, L. Rubio, R. Marcos, M. Dorn, C. Merker, I. Estrela-Lopis, M.R. Cimpan, M. Ibrahim, E. Cimpan, M. Ostermann, A. Sauter, N. El Yamani, S. Shaposhnikov, S. Chevillard, V. Paget, R. Grall, J. Delic, F. Goñi-De-Cerio, B. Suarez-Merino, V. Fessard, K.N. Hogeveen, L.M. Fjellsbo, E.R. Pran, T. Brzicova, J. Topinka, M.J. Silva, P.E. Leite, A.R. Ribeiro, J.M. Granjeiro, R. Grafström, A. Prina-Mello, M. Dusinska, High throughput toxicity screening and intracellular

- detection of nanomaterials, *WIREs Nanomed. Nanobiotechnol.* 9 (2016), <https://doi.org/10.1002/wnan.1413>.
- [26] H. Ruh, B. Kühn, G. Brenner-Weiss, C. Hopf, S. Diabaté, C. Weiss, Identification of serum proteins bound to industrial nanomaterials, *Toxicol. Lett.* 208 (2012) 41–50, <https://doi.org/10.1016/j.toxlet.2011.09.009>.
- [27] P. Aggarwal, J.B. Hall, C.B. Mcleland, M.A. Dobrovolskaia, S.E. Mcneil, NIH public access, *Science* 61 (2013) 428–437, <https://doi.org/10.1016/j.addr.2009.03.009>. Nanoparticle.
- [28] Z. Magdolenova, M. Drlickova, K. Henjum, E. Rundén-Pran, J. Tulinska, D. Bilanicova, G. Pojana, A. Kazimirova, M. Barancokova, M. Kuricova, A. Liskova, M. Staruchova, F. Ciampor, I. Vavra, Y. Lorenzo, A. Collins, A. Rinna, L. Fjellsbo, K. Volkovova, A. Marcomini, M. Amiry-Moghaddam, M. Dusinska, Coating-dependent induction of cytotoxicity and genotoxicity of iron oxide nanoparticles, *Nanotoxicology* 9 (2015) 44–56, <https://doi.org/10.3109/17435390.2013.847505>.
- [29] A. Kermanizadeh, S. Vranic, S. Boland, K. Moreau, A. Baeza-Squiban, B.K. Gaiser, L.A. Andrzejczuk, V. Stone, An in vitro assessment of panel of engineered nanomaterials using a human renal cell line: cytotoxicity, pro-inflammatory response, oxidative stress and genotoxicity, *BMC Nephrol.* 14 (2013) 96, <https://doi.org/10.1186/1471-2369-14-96>.
- [30] I. Pujalté, I. Passagne, B. Brouillaud, M. Tréguer, E. Durand, C. Ohayon-Courtès, B. L'Azou, Cytotoxicity and oxidative stress induced by different metallic nanoparticles on human kidney cells, *Part. Fibre Toxicol.* 8 (2011) 10, <https://doi.org/10.1186/1743-8977-8-10>.
- [31] F.A. Ding, Y.P. Li, J. Liu, L. Liu, W.M. Yu, Z. Wang, H.F. Ni, B.C. Liu, P.S. Chen, Overendocytosis of gold nanoparticles increases autophagy and apoptosis in hypoxic human renal proximal tubular cells, *Int. J. Nanomed.* 9 (2014) 4317–4330, <https://doi.org/10.2147/ijn.s68685>.
- [32] I. Passagne, M. Morille, M. Rousset, I. Pujalté, B. L'Azou, Implication of oxidative stress in size-dependent toxicity of silica nanoparticles in kidney cells, *Toxicology* 299 (2012) 112–124, <https://doi.org/10.1016/j.tox.2012.05.010>.
- [33] X. Valentini, L. Absil, G. Laurent, A. Robbe, S. Laurent, R. Muller, A. Legrand, D. Nonclercq, Toxicity of TiO₂ nanoparticles on the NRK52E renal cell line, *Mol. Cell. Toxicol.* 13 (2017) 419–431, <https://doi.org/10.1007/s13273-017-0046-1>.
- [34] A.A. Dayem, M.K. Hossain, S. Bin Lee, K. Kim, S.K. Saha, G.M. Yang, H.Y. Choi, S.G. Cho, The role of reactive oxygen species (ROS) in the biological activities of metallic nanoparticles, *Int. J. Mol. Sci.* 18 (2017) 1–21, <https://doi.org/10.3390/ijms18010120>.
- [35] R.J. Delfino, C. Sioutas, S. Malik, Potential role of ultrafine particles in associations between airborne particle mass and cardiovascular health, *Environ. Health Perspect.* 113 (2005) 934–946, <https://doi.org/10.1289/ehp.7938>.
- [36] K. Bedard, K.-H. Krause, The NOX family of ROS-Generating NADPH oxidases: physiology and pathophysiology, *Physiol. Rev.* 87 (2007) 245–313, <https://doi.org/10.1152/physrev.00044.2005>.
- [37] M. Valko, C.J. Rhodes, J. Moncol, M. Izakovic, M. Mazur, Free radicals, metals and antioxidants in oxidative stress-induced cancer, *Chem. Biol. Interact.* 160 (2006) 1–40, <https://doi.org/10.1016/j.cbi.2005.12.009>.
- [38] P. Dua, K.N. Chaudhari, C.H. Lee, N.K. Chaudhari, S.W. Hong, J.S. Yu, S. Kim, D.K. Lee, Evaluation of toxicity and gene expression changes triggered by oxide nanoparticles, *Bull. Korean Chem. Soc.* 32 (2011) 2051–2057, <https://doi.org/10.5012/bkcs.2011.32.6.2051>.
- [39] H.S. Choi, W. Liu, P. Misra, E. Tanaka, J.P. Zimmer, B. Itty Ipe, M.G. Bawendi, J.V. Frangioni, Renal clearance of nanoparticles, *Nat. Biotechnol.* 25 (2007) 1165–1170, <https://doi.org/10.1038/nbt1340>. Renal.
- [40] B. Du, M. Yu, J. Zheng, Transport and interactions of nanoparticles in the kidneys, *Nat. Rev. Mater.* 3 (2018) 358–374, <https://doi.org/10.1038/s41578-018-0038-3>.
- [41] J.E. Zuckerman, A. Gale, P. Wu, R. Ma, M.E. Davis, siRNA delivery to the glomerular mesangium using polycationic cyclodextrin nanoparticles containing siRNA, *Nucleic Acid Ther.* 25 (2015) 53–64, <https://doi.org/10.1089/nat.2014.0505>.
- [42] R.M. Williams, J. Shah, H.S. Tian, X. Chen, F. Geissmann, E.A. Jaimes, D.A. Heller, Selective nanoparticle targeting of the renal tubules, *Hypertension* 71 (2018) 87–94, <https://doi.org/10.1161/HYPERTENSIONAHA.117.09843>.
- [43] F. Oroojalian, A.H. Rezayan, F. Mehrnejad, A.H. Nia, W.T. Shier, K. Abnous, M. Ramezani, Efficient megalin targeted delivery to renal proximal tubular cells mediated by modified-polymyxin B-polyethylenimine based nano-gene-carriers, *Mater. Sci. Eng. C* 79 (2017) 770–782, <https://doi.org/10.1016/j.msec.2017.05.068>.
- [44] N. Oh, J.H. Park, Endocytosis and exocytosis of nanoparticles in mammalian cells, *Int. J. Nanomed.* 9 (2014) 51–63, <https://doi.org/10.2147/IJN.S26592>.
- [45] B. Buliaková, M. Mesárošová, A. Bábelová, M. Šelc, V. Némethová, L. Šebová, F. Rážga, M. Ursínyová, I. Chalupa, A. Gábelová, Surface-modified magnetite nanoparticles act as aneugen-like spindle poison, *Nanomed. Nanotechnol. Biol. Med.* 13 (2017) 69–80, <https://doi.org/10.1016/j.nano.2016.08.027>.
- [46] H.L. Karlsson, S. Di Bucchianico, A.R. Collins, M. Dusinska, Can the comet assay be used reliably to detect nanoparticle-induced genotoxicity? *Environ. Mol. Mutagen.* 56 (2015) 82–96, <https://doi.org/10.1002/em.21933>.